Electrochemical Hydrogen Storage Behaviors of Ultrafine Amorphous Co−B Alloy Particles

Ya D. Wang, Xin P. Ai, and Han X. Yang*

Department of Chemistry, Wuhan University, Wuhan 430072, China

Received May 12, 2004. Revised Manuscript Received August 27, 2004

Ultra-fine amorphous alloy particles (UAAP) of Co−B were synthesized and investigated as an anode material in aqueous KOH solution. The experimental results demonstrated that the Co−B particles so prepared show excellent electrochemical reversibility and considerably high charge−discharge capacity. The reversible discharge capacity of the Co−B UAAP electrode is found to exceed 300 mAh/g at a current rate 100 mA/g, similar to values for conventional hydrogen storage alloys. In addition, the cycling ability and high rate capability of the Co−B electrode are fairly good with only 10% capacity decay after 100 cycles at a high rate of 300 mA/g. These exceptional electrochemical performances are suggested to arise from the electrochemical hydrogen storage reaction on the Co−B material, which is brought about by the nanosize effects and special amorphous structure of the Co−B UAAP particles.

Introduction

Hydrogen storage alloys (HMs) have been actively investigated as a high capacity negative material of nickel−metal hydride batteries for use in various electronic devices and hybrid low-emission vehicles.[1−3] In the past few decades, many metal hydrides, such as AB_5-type rare-earth metal alloys,[4−10] AB_2-type Laves phase alloys,[11,12] A_2B-type Mg-based alloys,[13,14] and AB-type intermetallic compounds,[15,16] have been explored, and a large amount of work, such as the optimization of alloy composition[17−20] and surface modifications,[21−23] has been done to improve the electrochemical capacity and high rate capability of these materials. Though some of the Mg-based alloys have very high capacities of ≥600 mAh/g, their cycling abilities and poor dynamics are insufficient for practical applications.[24,25] At the present state of the art, the commercially used MHs usually have a reversible capacity of ∼300 mAh/g,[26,27] and therefore, the search for new hydrogen storage materials with higher energy density has been continuously carried out in recent years.

Nanosized materials have received considerable interest for development of new generation of hydrogen storage materials because of their unique characteristics[28] such as high surface reactivity and strong gas adsorption. Carbon nanotubes[29−33] and some nanosized alloy particles[34−37] were reported to have larger hydro-

* Corresponding author. Phone: +86-027-87873526. Fax: +86-027-87884476. E-mail: ece@whu.edu.cn.

(1) Köhler, U.; Kümper, J.; Ullrich, M. *J. Power Sources* **2002**, *105*, 139−134.
(2) Bor Yann, L.; Yang, x.-G. *Solid State Ionics* **2002**, *152−153*, 217−225.
(3) Jiang, J.-J.; Gasik, M.; Laine, J.; Lampinen, M. *J. Alloys Compd.* **2001**, *322*, 281−285.
(4) Yuexiang, H.; Hong, Z. *J. Alloys Compd.* **2000**, *305*, 76−81.
(5) Jain, I. P.; Abu Dakka, M. I. S. *Int. J. Hydrogen Energy* **2002**, *27*, 395−401.
(6) Yamamoto, M.; Kanda, M. *J. Alloys Compd.* **1997**, *253−254*, 660−664.
(7) Li, C.-J.; Wang, X.-L. *J. Alloys Compd.* **1999**, *284*, 274−281.
(8) Meli, F.; Sakai, T.; Zutel, A.; Schlapbach, L. *J. Alloys Compd.* **1995**, *221*, 284−290.
(9) Hsu, S. E.; Beibutian, V. M.; Yeh, M. T. *J. Alloys Compd*. **2002**, *330−332*, 882−885.
(10) Jensen, J. O.; Bjerrum, N. J. *J. Alloys Compd*. **1999**, *293−295*, 185−189.
(11) Lee, H.; Lee, S.-M.; Lee, J.-Y. *J. Electrochem. Soc.* **1999**, *146* (10), 3666−3671.
(12) Song, M. Y.; Ahn, D.; Kwon, I. H.; Chough, S. H. *J. Electrochem. Soc*. **2001**, *148* (9), A1041−A1044.
(13) Akiyama, T.; Saito, K.; Saita, I. *J. Electrochem. Soc*. **2003**, *150* (9), E450−E454.
(14) Sakaguchi, H.; Kohzai, A.; Hatakeyama, K.; Fujine, S.; Yoneda, K.; Kanda, K.; Esaka, T. *Int. J. Hydrogen Energy* **2000**, *25*, 1205−1208.
(15) Yukawa, H.; Takahashi, Y.; Morinaga, M. *Comput. Mater. Sci.* **1999**, *14*, 291.
(16) Yukawa, H.; Takahashi, Y.; Morinaga, M. *Comput. Mater. Sci.* **1999**, *14*, 291−294.
(17) Vivet, S.; Joubert, J.-M.; Knosp, B.; Percheron-Guegan, A. *J. Alloys Compd*. **2003**, *356−357*, 779−783.
(18) Yuexiang, H.; Hui, Y.; Hong, Z. *J. Alloys Compd*. **2002**, *330−332*, 831−834.
(19) Fukumoto, Y.; Miyamto, M.; Inoue, H.; Masuoka, M.; Iwakura, C. *J. Alloys Compd*. **1995**, *231*, 562−564.
(20) Iwakura, C.; Okura, T.; Inoue, H.; Matsuoka, M.; Yamamoto, Y. *J. Electroanal. Chem.* **1995**, *398*, 37−41.
(21) Lee, S.-M.; Park, J.-G.; Han, S.-C.; Lee, P. S.; Lee, J.-Y. *J. Electrochem. Soc*. **2002**, *149* (10), A1278−A1281.
(22) Yang, H.; Ji, J.; Sun, H.; Yuan, H.; Zhou, Z.; Zhang, Y. *J. Electrochem. Soc*. **2001**, *148* (6) A554−A558.
(23) Chen, W. X.; Xu, Z. D.; Tu, J. P. *Int. J. Hydrogen Energy* **2002**, *27*, 439−444.
(24) Hong, T.-W.; Kim, Y. J. *J. Alloys Compd*. **2002**, *333*, L1−L6.
(25) Dehouche, Z.; Goyette, J.; Bose, T. K.; Schulz, R. *Int. J. Hydrogen Energy* **2003**, *28*, 983−988.
(26) Hu, W.-K. *J. Alloys Compd*. **2000**, *297*, 206−210.
(27) Köhlerm, U.; Kümpers, J.; Ullrich, M. *J. Power Sources* **2002**, *105*, 139−144.
(28) Gleiter, H. *Prog. Mater. Sci.* **1988**, *233*, 223−315.
(29) − Baughman, R. H.; Zakhidov, A. A.; de Heer, W. A. *Science* **2002**, *297*, 789−790.
(30) Liu, C.; Fan, Y. Y.; Liu, M.; Cong, H. T.; Cheng, H. M.; Dresselhaus, M. S. *Science* **1999**, *286*, 1127−1129.
(31) Dillon, A. C.; Jones, K. M.; Bekkendahl, T. A.; Kiang, C. H.; Bethune, D. S.; Heben, M. J. *Nature* **1997**, *386*, 377.
(32) Lombardi, I.; Bestetti, M.; Mazzocchia, C.; Cavallotti, P. L.; Ducati, U. *Electrochem. Solid-State Lett.* **2004**, *7* (5), A115−A118.
(33) Dai, G. P.; Liu, M.; Chen, D. M.; Xiang, P.; Hou, Y. T.; Cheng, H. M. *Electrochem. Solid-State Lett.* **2002**, *5* (4), E13−E15.

10.1021/cm049252f CCC: $27.50
Published on Web 10/09/2004

gen storage capacities than conventional hydrogen absorbing alloys; however, the room temperature kinetic behaviors of these materials are not satisfactory. In this paper, we report the electrochemical hydrogen storage behaviors of the Co−B UAAP synthesized by chemical reduction of cobalt in aqueous borohydride solution and describe the charge−discharge properties of this material used as a hydrogen storage electrode.

Experimental Section

2.1. Material Synthesis. The ultra-fine amorphous Co−B alloy particles were synthesized by chemical reduction of cobalt sulfate in aqueous sodium borohydride solution. The synthetic apparatus and experimental manipulations were performed almost in the same way as described in ref 38, and the only difference is that we used an ice bath to control the reaction temperature rather than using circulating isothermal water. A typical experimental procedure is as follows: 250 mL of sodium borohydride solution (0.5 mol L^{-1}) was first prepared and adjusted to pH = 12 with sodium hydroxide to prevent violent hydrolysis. Bivalent cobalt sulfate solution (0.1 mol L^{-1}, 250 mL) was prepared with degassed distilled water and then cooled in an ice bath. The chemical reduction reaction was carried out by adding borohydride solution dropwise into $CoSO_4$ solution at stirring. When the addition was complete, the solution bath was kept at stirring about 1 h to release the hydrogen to prevent burning of the precipitate following filtration. After that, the precipitate was washed first with distilled water to remove the reaction residues, and then with acetone to prevent the sample surface from further oxidizing. Finally, the sample was dried in a vacuum at 80 °C for 14 h for the removal of residual water and acetone. All the reagents were of analytical grade (Shanghai Chemical Reagent Company) and used as received without further purification.

2.2. Electrochemical Measurements. The cyclic voltammetry (CV) was conducted by using a powder microelectrode. The powder microelectrode was fabricated in a similar way as described in ref 39 by filling the Co−B alloy particles into a microcavity at the tip of a Pt microdisk electrode. A Hg/HgO electrode in 30% KOH was used as reference electrode, and a sintered nickel hydroxide electrode was used as counter electrode. The potential scan rate was set to 2 mV/s.

The Co−B electrode used for charge−discharge experiments was a porous membrane electrode, prepared first by mixing 85% Co−B alloy powders, 7% poly(tetrafluoroethylene) (in emulsion) and 8% acetylene black into paste, then by roll-pressing the paste to 0.15 mm thick films, and finally by pressing the film onto a nickel mesh. The experimental cell was constructed with a 4 cm^2 Co−B electrode as anode, a sintered nickel electrode as cathode, and 30% KOH solution as electrolyte.

2.3. Compositional and Structural Characterization. The size and morphology of the Co−B alloy particles were examined by transmission electron microscopy (TEM) on a JEM-2010 microscope. The crystalline structures of Co−B alloy particles were characterized by powder X-ray diffractometry (XRD) on a Shimadzu Lab diffractometer with Cu Kα source. The electrode samples for characterization of the changes in the crystalline phases at different charge and discharge states were taken from the cells, rinsed with distilled water, and then dried for direct ex-situ XRD analysis. The chemical composition of the Co−B alloy particles was determined by inductively coupled plasma (ICP) analysis using a JY38S spectrometer.

(34) Fujiia, H.; Orimo, S.-i. *Physica B* **2003**, *328*, 77−80.
(35) Jurczyk, M. *J. Alloys Compd*. **2000**, *307*, 279−282.
(36) Tanaka, K.; Sowa, M.; Kita, Y.; Kubota, T.; Tanaka, N. *J. Alloys Compd*. **2002**, *330−332*, 732−737.
(37) Kronberger, H. *J. Alloys Compd*. **1997**, *253−254*, 87−89.
(38) Shen, J.; Li, Z.; Yan, Q.; Chen, Y. *J. Phys. Chem*. **1993**, *97*, 8504−8511.
(39) Cha, C. S.; Li, C. M.; Yang, H. X.; Liu, P. F. *J. Electroanal. Chem*. **1994**, *368*, 47−54.

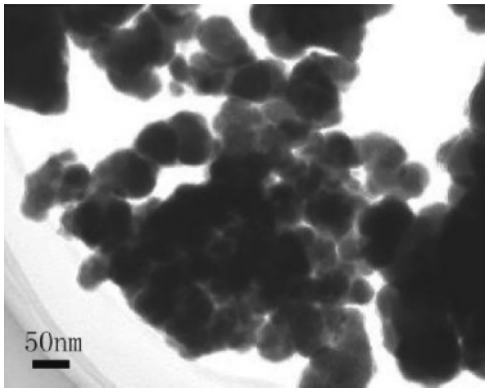

Figure 1. TEM micrograph of the Co−B UAAP powder.

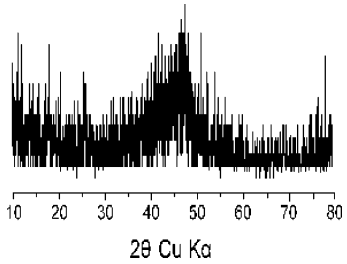

Figure 2. XRD patterns of the Co−B UAAP powder

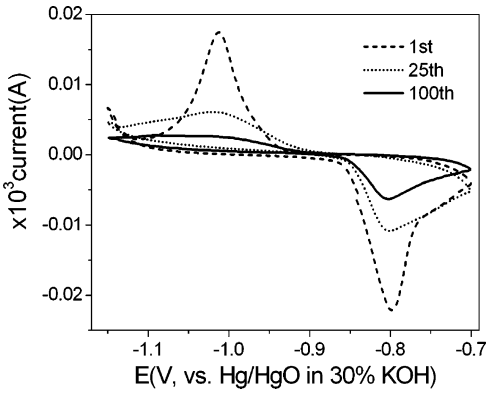

Figure 3. Typical CV curves of the Co−B UAAP electrode in a 30% KOH solution. Potential sweep rate was set at 2 mV/s.

Results and Discussion

3.1. Material Characterization. The Co−B alloy particles prepared in this work have a Co/B atomic ratio of 1.9, approximately. Figures 1 and 2 show the HRTEM image and XRD pattern of the Co−B powers prepared in this work, respectively. As it is shown in Figure 1, the Co−B powers consist of very fine particles with almost uniform size of several tens of nanometers, resembling very much what was reported previously in ref 38. In the previous work,[38] it is clearly demonstrated by the TEM micrograph together with an electron-diffraction image that the Co−B particles so prepared had an ultrafine amorphous structure. In addition, the very weak and featureless XRD pattern in our work (Figure 2) further confirms the amorphous crystalline structure of the Co−B particles synthesized by this method.

3.2. Electrochemical Characterization. Figure 3 shows the cyclic voltammograms of the Co−B powders in 30% KOH aqueous solution. During first cathodic scan, a remarkable reduction peak appears at −1.01 V, and correspondingly, a strong oxidation peak arises at

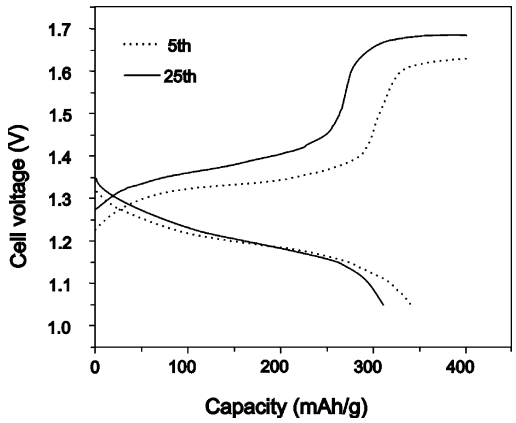

Figure 4. Charge and discharge curves of the Co−B UAAP electrode at a constant current of 100 mA/g.

the more positive potential of −0.8 V on the anodic branch of the CV curve. This pair of the reduction−oxidation peaks suggests a reversible electrochemical reaction occurring on the Co−B UAAP electrode. From the thermodynamic point of view, the equilibrium potentials of elemental cobalt and boron are at −0.733 and −1.811 V, respectively, in the alkaline solution,[40] which are far from the potential locations for the observed current peaks in Figure 3, and therefore, the pair of current peaks cannot be accounted for by a simple electrochemical reduction and oxidation of the elemental cobalt or boron in the Co−B UAAP electrode. Considering that the potential positions and shapes of these current peaks very well resemble those frequently observed for the electrochemical hydrogen storage reactions on MH electrodes,[41] we can attribute the current peaks to the electrochemical reduction of H_2O and the oxidation of absorbed hydrogen on the Co−B electrode. A conflicting phenomenon in Figure 3 is that the anodic peak is somewhat larger than the anodic current peak, implying that the oxidation capacity given by the absorbed hydrogen exceeds the reduction capacity used for the generation of hydrogen in the first cycle of potential scan. This problem is probably due to the residual hydrogen, which is formed in the chemical precipitation of Co−B by borohydride reduction and strongly absorbed in the crystalline lattice of Co−B particles. This phenomenon also suggests the possibility that the Co−B UAAP could react with hydrogen atoms to form a hydride alloy since the residual hydrogen should be completely removed during vacuum-drying of the material at 80 °C, if hydrogen exists in a physically adsorbed state.

To ensure the practical feasibility of the Co−B UAAP as a hydrogen storage electrode material, we constructed the experimental Ni−MH cells using the Co−B negative electrodes and $Ni(OH)_2$ positive electrodes, and cycled the cells at conventional charge−discharge conditions. Figure 4 shows the charge−discharge curves of the cells at a constant current of 100 mA/g. As it is shown, the charging and discharging curves of the cells are almost the same as usually observed for the Ni−MH cells based on conventional hydrogen storage alloys;[41] i.e., the charging and discharging voltage plateaus appear just at the potentials of ∼1.2 and ∼1.35 V, respectively, which are characteristic of the reversible electrochemical storage and oxidation of hydrogen. Calculated from the discharge curves in Figure 4, the discharge capacity of the Co−B electrode is ca. 340 mAh/g at the fifth cycle and 310 mAh/g at the 25th cycle, slightly higher than the electrochemical capacities of the rare-earth metal alloys currently used in commercial Ni−MH batteries.[41]

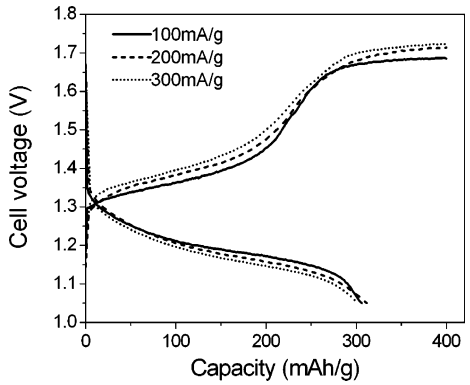

Figure 5. Comparison of the charge−discharge curves of the Co−B UAAP electrode at different current rates and at the fifth cycle.

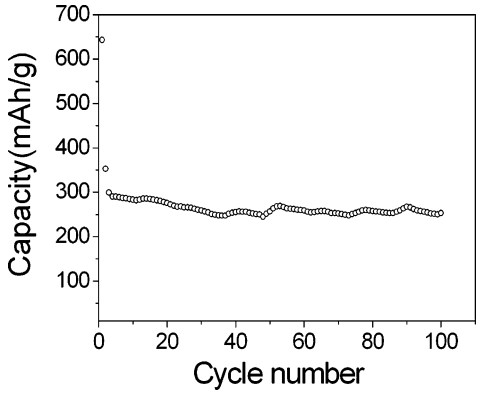

Figure 6. Cycling performance of the Co−B UAAP electrode at a rate of 300 mA/g.

The rate capability of the Co−B electrode can be seen from the charge−discharge curves at different current rate as shown in Figure 5. It can be seen that there is no obvious decrease in the discharge capacities and voltage plateaus at increased discharge rates. The discharge capacity of the Co−B electrode at the high rate of 300 mA/g is also almost the same as at the rate of 100 mA/g current, suggesting that the Co−B UAAP electrode can not only serve as "high capacity anode", but also serve as "high power capability anode".

Figure 6 shows the cycling performances of the Co−B electrode at a high rate of 300 mA/g. At the initial cycle, the Co−B electrode shows an exceptionally high irreversible discharge capacity of ca. 600 mA/g, possibly due to the electrochemical oxidation of boron and active surface cobalt atoms. From the third cycle, the reversible capacity was stabilized at ca. 300 mA/g. Even after 100 cycles, the reversible capacity was still kept up at more than 260 mAh/g, showing quite good capacity retention.

Usually, most of the conventional hydrogen storage alloys need an electrochemical activation process to achieve their intrinsic hydrogen storage capabilities.[11]

(40) Bard, A. J.; Parsons, R.; Jordan, J. *Standard Potentials in Aqueous Solution*; Marcel Dekker, Inc.: New York, 1985.
(41) Hong, K. *J. Alloys Compd*. **2001**, *321*, 307−313.

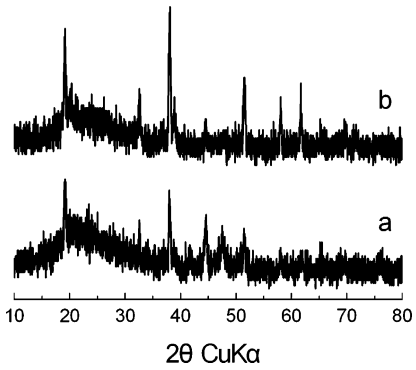

Figure 7. XRD patterns of the Co−B UAAP electrode: (a) fully charged and (b) completely discharged at the 20th cycle.

In comparison, the Co−B UAAP material shows an exceptional electrochemical activity and can work very well without the need of any chemical or electrochemical preactivation treatments. This is particularly beneficial for practical hydrogen storage or battery applications.

3.3. Electrode Reaction Mechanism. To confirm the charge−discharge mechanism of the Co−B electrode as suggested above, we used XRD and XPS spectroscopy to characterize the changes in the chemical composition and electronic structure of the Co−B electrode during charge−discharge cycling. Figure 7 compares the XRD patterns of the Co−B electrode from fully charged and discharged cells. In the figure, a number of very weak XRD lines, which can all be indexed to β-$Co(OH)_2$, are observed from both the charged and discharged surfaces of the electrode. Because these XRD peaks are too weak and do not change very much in the charged or discharged electrode, it is difficult to assign these peaks to the phase transformation of the electrode from amorphous Co−B particles to crystalline β-$Co(OH)_2$. Most likely, these XRD features are given rise by the surface oxide of cobalt, produced during the sample preparation or by chemical corrosion of the electrode in alkaline solution. Nevertheless, the failure to observe the phase change of the electrode during charge−discharge cycling seems to support the electrochemical hydrogen storage mechanism. In addition, we also failed to detect any significant changes in the electronic valence state of cobalt in the electrode during charge and discharge.

It has been well recognized that cobalt can form a solid solution with hydrogen with the atomic ratio of hydrogen to cobalt up to 1.[42] If the Co−B alloy is hydrogenated to form Co_2BH_2, the theoretical special capacity of the Co−B particles should be 414 mAh/g. However, there were always some borate residues or surface oxides (totally, ca. 10% by ICP measurements) existing in the Co−B product, which cannot form hydride and would certainly lead to a reduction of the observed capacity from its theoretical value; thus, the observation of 300 mAh/g reversible capacity for the Co−B alloy particles is reasonable.

The excellent cycle life of the Co−B alloy is most likely due to the stable amorphous structure of this compound. As shown above, no significant phase transformation or bulk oxidation occurs in the Co−B alloy particles during charge and discharge cycles. This exceptional oxidation-resistant property of the Co−B particles may arise from the alloying effect of Co with B atoms, which leads to the electrode potential ≤ 1.0 V of the alloy being much more negative than that of the pure Co element (−0.73). As a consequence, the oxidative passivation of the Co in the Co−B alloy particles is greatly alleviated.

Conclusion

In summary, we synthesized the ultra-fine amorphous alloy Co−B particles through borohydride reduction of divalent cobalt and investigated the structural and electrochemical properties of this material used as a rechargeable anode electrode in aqueous KOH solution. The reversible discharge capacity of the Co−B UAAP electrode is obtained as more than 300 mAh/g at a rate of 100 mA/g current, comparable to those of conventional hydrogen storage alloys. In addition, the cycling ability and high rate capability of the Co−B electrode are fairly good with only 10% capacity decay after 100 cycles at a high rate of 300 mAh/g. The exceptional electrochemical activities of the Co−B UAAP material were explained by an electrochemical hydrogen storage reaction, which is brought about by the high chemical reactivity and special amorphous structure of the nanosized particles.

Acknowledgment. The authors acknowledge financial support by the 973 Program, China (Grant 2002CB-211800).

CM049252F

(42) Antonov, V. E.; Antonova, T. E.; Baier, M.; Grosse, G.; Wagner, F. E. *J. Alloys Compd*. **1996**, *239*, 198.